

Studies on the N-terminal motif of PMP70 that suppresses
cotranslational targeting to the endoplasmic reticulum
「合成と共役した小胞体標的化を抑制するPMP70のN末端モチ
ーフに関する研究」

2015

阪上春花

兵庫県立大学大学院生命理学研究科

Studies on the N-terminal motif of PMP70 that suppresses
cotranslational targeting to the endoplasmic reticulum

2015

Haruka Sakaue

Department of Life Science
Graduate School of Life Science University of Hyogo

Contents

1. Abstract	3
2. Introduction	4
3. Abbreviations	6
4. Materials and methods	7
4.1. Materials	
4.2. DNA construction	
4.3. <i>In vitro</i> translation and assessment of ER translocation	
4.4. Expression and topology analysis in COS7 cells	
4.5. Purification of N12-GST fusion protein and competition assay	
4.6. Sucrose density gradient centrifugation and crosslinking experiments with the N12-RNC	
4.7. Immunofluorescence microscopy of full-length PMP70	
5. Results	12
5.1. ER integration of TM1 is suppressed by an upstream 80-residue segment	
5.2. N-terminal short motif suppresses the translocation by TM1 into the ER membrane	
5.3. Ser ⁵ is essential for ER-targeting suppression	
5.4. Importance of the N-terminal region was confirmed in the cells.	
5.5. A short motif can suppress the signal peptide function of pre-prolactin	
5.6. N12 is effective only at the N-terminus of the nascent chain	
5.7. N12 function was competitively inhibited by N12-fusion protein	
5.8. The 50-kDa and the 20-kDa factors were crosslinked with the N12-nascent chains	
5.9. S5A mutation caused mislocation of PMP70 to the ER in cultured cells	
6. Discussion	31
7. References	34
8. Acknowledgments	39
9. Supplemental figures	40

1. Abstract

Many membrane proteins possessing hydrophobic transmembrane segments are cotranslationally integrated into the ER membrane. Various peroxisomal and mitochondrial membrane proteins escape the ER-targeting mechanism and are targeted to their destinations. Here I discovered a short segment in the 70-kDa peroxisomal membrane protein (PMP70) that suppresses ER targeting. The first transmembrane segment has an intrinsic signal function that targets the nascent chain to the ER. The ER-targeting was suppressed by a short N-terminal sequence of 9 residues that is 80 residues upstream of the transmembrane segment. Among the 9 residues, Ser⁵ is indispensable. The short segment also suppressed the signal peptide function of an authentic secretory protein. This function of the short segment was suppressed by the recombinant motif-GST fusion protein. The 50-kDa and 20-kDa proteins were crosslinked with the motif. The PMP70 molecule with the Ser5Ala point mutation predominantly localized to the ER. I propose the concept of an ER-targeting suppressor that suppresses the ER-targeting mechanism via a binding factor.

2. Introduction

Most integral membrane proteins in the secretory pathways in eukaryotic cells are cotranslationally integrated into the ER membrane. During the process, hydrophobic transmembrane (TM) segments of the membrane proteins emerging from the ribosome are recognized by the signal recognition particle (1). The nascent polypeptide chain is then targeted to the ER via the signal recognition particle receptor, and transferred to a protein translocation channel that comprises a Sec61 complex (2). The signal recognition particle and Sec61 complex recognize the hydrophobic nature of the polypeptide chain. Thus, TM segments of general membrane proteins tend to be targeted to the ER. On the other hand, mitochondrial and peroxisomal membrane proteins must escape the ER-targeting mechanism. Although various organelle-targeting sequences have been characterized to date, the fundamental issue of how hydrophobic segments of peroxisomal membrane proteins are not targeted to the ER membrane has not been elucidated. I hypothesized that the ER-targeting mechanism is modulated by a cis-acting sequence upstream of the hydrophobic TM segment.

Isoforms of the ABC transporter family are ideal for studying the sorting process of highly hydrophobic membrane proteins, because although they possess similarly hydrophobic TM segments, the various isoforms are localized to specific organelle membranes (3). Mitochondrial localization of the ABC transporter isoform ABCB10 has been investigated (4,5). ABCB10 possesses a long 105-residue presequence that suppresses cotranslational ER-targeting and switches the targeting mechanism to posttranslational mitochondrial targeting. In the absence of the presequence, the membrane domain of the B10 isoform is cotranslationally integrated into the ER membrane (4). It cannot be functionally replaced with other short presequences of matrix-soluble proteins. The strong mitochondrial targeting property is essential for suppressing the ER-targeting of the hydrophobic membrane domain. Other mitochondrial isoforms, B7 and B8, possess similar long presequences.

Peroxisomal membrane proteins (PMP), including the ABC transporter family, also

possess hydrophobic TM segments but are able to escape ER-targeting. Multispanning PMPs possess multiple peroxisomal targeting signals in a single polypeptide chain (6-8). The 70-kDa major peroxisomal membrane protein (PMP70, ABCD3 isoform) (9) possesses two distinct peroxisome targeting signals in the N-terminal region (Met¹-Arg¹²⁴), including TM1 and TM2, and the middle region (Glu²⁶⁴-Val³⁷⁵) including TM5 and TM6 (10). Pex19, a peroxisome-assembly factor, binds multiple sites of peroxisomal membrane proteins and maintains them in a soluble form before import into the peroxisomal membrane (11-14). Pex19 binding sites of PMP70 exist in the Met¹-Arg⁶¹ and Gly²⁶³-Lys³⁴⁷ regions, including TM5 and TM6 (15). In the absence of Pex19, the PMP70 molecule is not imported into the peroxisome, but is instead rapidly degraded in the cytosol (16). In our recent study, we revealed that the N-terminal region (Met¹-Cys⁸⁰) possesses a mitochondrial targeting function and is integrated into the mitochondrial outer membrane by itself (17).

Here I demonstrated that TM1 possesses a signal function sufficient to mediate the insertion of a polypeptide chain into the ER and that this function is suppressed by the 80 upstream residues. A short N-terminal motif is critically involved in suppressing the ER-targeting of TM1. The short motif also suppresses ER-targeting of the secretory protein prolactin. Unexpectedly, the Ser⁵ in the motif is essential and could not be replaced by any other residue. This is a novel cis-acting element that suppresses ER-targeting whose function depends on a specific amino acid residue. Peptide competition experiments and crosslinking analysis strongly suggested that the specific recognition of a saturable factor is involved in this process.

3. Abbreviations

BMOE, bismaleimidoethane

DMEM, Dulbecco's modified Eagle's medium

EndoH, endoglycosidase H

ETS, ER-targeting suppressor

FCS, fetal calf serum

PMP, peroxisomal membrane proteins

PMP70, 70-kDa peroxisomal membrane protein

pPL, pre-prolactin

PLg, glycosylatable prolactin

ProK, proteinase K

RM, rough microsomal membrane

RNC, ribosome nascent chain complex

TCA, trichloroacetic acid

TM, transmembrane

4. Materials and methods

4.1. Materials

Rabbit anti-Pex14 antibodies were a generous gift from Dr. Komori of Osaka Prefecture University. The RM (18) and reticulocyte lysate (19) were prepared as previously described. ProK (Merck) was dissolved in 10 mM HEPES (pH 7.4) at 2 mg/ml and stored in a freezer in small aliquots until use. EndoH fusion protein and prestained protein markers were obtained from New England BioLabs. FuGENE6 (Promega), digitonin (Wako Chemicals), wheat germ extract for cell-free translation (Promega), mouse anti-HA monoclonal antibody (Covance), rabbit anti-PL antiserum (Merck-Millipore), MG132 (Sigma-Aldrich), and BMOE (Thermo) were purchased from the companies indicated. The expression plasmid of EGFP-Cytb5 and rabbit anti-EGFP antibodies were described (20,21).

4.2. DNA construction

PCR-generated DNA fragments and plasmid DNA were digested by the restriction enzymes indicated in the parentheses and ligated. For *in vitro* transcription and translation experiments, I used the pSPBP4 (22) plasmid with the SP6 RNA polymerase promoter and a *Xenopus* β -globin 5'-noncoding sequence. Point mutations and partial deletions were made using the Quikchange method (23). pSPBP4 was digested with NcoI and XhoI and the endogenous insert was removed. For the N-terminal fusion proteins shown in Figure 1B, DNA fragments (NcoI/XhoI) coding for segments of the PMP70 (Met¹-Glu¹¹¹, Met¹-Ser⁴⁰, Cys⁸⁰-Glu¹¹¹ [a Val residue was inserted between the initiation Met¹ and the Cys⁸⁰ residue]) and PLg cDNA (XhoI/XbaI) were ligated into the NcoI and XbaI sites of pSPBP4. For the deletion constructs shown in Figure 1C, DNA fragments coding for 60-111 (Asp⁶⁰-Glu¹¹¹, NcoI/XhoI) and 10-111 (Ala¹⁰-Glu¹¹¹, NcoI/XhoI) fusion proteins were subcloned into the pSPBP4 plasmid (NcoI/XhoI). Deletions of Δ SK, Δ SKYL, Δ 19-80, and Δ 10-79 were made using the Quikchange method. For the processing site mutant, the signal peptidase processing site

(Cys⁹⁹-Asp¹⁰⁰) was predicted by Signal-P server (24) and the point-mutant C99W was predicted to be a poor substrate. The processing mutant (C99W), the glycosylation site mutant (T108A), and the point mutants shown in Figure 2 were made using the Quikchange method. For the pre-prolactin fusion proteins shown in Figure 4, the N12-sequence and the N12(S5A)-sequence were fused to the N-terminus of pre-prolactin in pSPBP4 using the Quikchange method. Glycine insertions were also made from N12-pPL constructs using the Quikchange method. For expression in COS cells (Figs. 3 and 4), DNA fragments encoding the 1-111 fusion proteins and the pPL constructs were subcloned downstream of the CMV promoter of pRcCMV (HindIII/XbaI). For GST fusion constructs, DNA fragments encoding the N-terminal 14 residues of PMP70 or its S5A mutant (NdeI/XhoI) and GST (XhoI/BamHI) was subcloned between the NdeI and BamHI sites of pET3a (Novagen). To make the ribosome-nascent chain complex, the plasmid in which N12-pPL and the S5A mutant were cloned in the pRcCMV vector was linearized at the Asn97 codon of pPL-coding sequence with PvuII. For expression of the full-length PMP70, human PMP70 cDNA (HindIII/NheI) was subcloned between the HindIII and XbaI sites of pRcCMV-HA (25). All the constructed DNAs were confirmed by DNA sequencing.

4.3. *In vitro* translation and assessment of ER translocation

Template plasmid DNA was linearized with XbaI and transcribed with SP6 RNA polymerase as described previously (26). *In vitro* protein synthesis and translocation experiments were performed essentially as described previously (27). All the translations included 10 µg/ml castanospermine, an inhibitor of glucosidase in the ER lumen, to reduce the heterogeneity of glycosylated bands due to sugar chain trimming (28). Because excess mRNA affected the ER targeting and translocation efficiency, I titrated the mRNA and used as little as possible for the translation. After the translation, aliquots were treated with ProK (500 µg/ml) on ice for 60 min. Other aliquots were treated with EndoH at 36°C for 1 h under denaturing conditions according

to the manufacturer's instructions. Radiolabeled proteins were analyzed by SDS-PAGE and visualized on a Bioimage analyzer BAS-1800 (Fuji Film). Quantification was performed using Image Gauge software (v4.0; Fuji Film). In the presence of RM, the products were processed and/or glycosylated to various extents. Protein bands were quantitated and the efficiencies of membrane insertion of the TM1 segment were estimated as the translocation % of the PLg domain according to the following formula: $(b+c) \times 100 / (a+b+c)$; the unprocessed-unglycosylated form (a); the unprocessed-monoglycosylated form (b); processed-diglycosylated form (c). The amounts of the processed-monoglycosylated and processed-unglycosylated forms were negligible.

4.4. Expression and topology analysis in COS7 cells

COS7 cells were maintained in DMEM supplemented with 10% FCS under 5% CO₂ atmosphere. Transfections using FuGENE 6 reagent were performed as described previously (21,29). The minimum amount of the expression plasmid required for immunoblotting detection was determined by titration. The transfected cells were cultured for 24 h. Where indicated, the proteasome inhibitor MG132 (10 μM) was included for 9 to 12 h before harvesting. For ProK treatment of organelle membranes, cells on a culture dish were permeabilized in permeabilizing buffer (20 mM HEPES–KOH [pH 7.5], 0.25 M sucrose, 2.5 mM magnesium acetate, 25 mM KCl, and 2.5 mM EGTA) containing 25 μg/ml digitonin at 26°C for 5 min, washed twice with the permeabilizing buffer, and then collected with a cell scraper (Corning). The permeabilized cells were resuspended in the permeabilizing buffer without digitonin and treated with ProK (60 μg/ml) on ice for 60 min either in the presence or absence of 1% Triton X-100. Other aliquots were treated with EndoH under denaturing conditions. The enzyme reactions were terminated with 10% TCA and the protein precipitates were washed with 80% acetone and then subjected to SDS-PAGE and immunoblotting analysis using anti-PL and HA antibodies.

4.5. Purification of N12-GST fusion protein and competition assay

The expression plasmid was transformed into BL21(DE3) strain. The expression was induced with IPTG for 2 h at 37°C. After disrupting the cells by sonication, the fusion proteins were recovered in the soluble fraction and purified using glutathione-agarose (Sigma). The protein was eluted with 10 mM reduced glutathione and the pure fractions were dialyzed with 20 mM HEPES/KOH (pH 7.5) using Tohrukun (Japan Genetics). For the N12-GST competition assay, translation reactions of the N12-pPL or 1-111 constructs were performed in the presence of various amounts of the purified N12-GST fusion proteins for 1 h at 30°C.

4.6. Sucrose density gradient centrifugation and crosslinking experiments with the N12-RNC

The template DNA harboring the N12-pPL constructs and the S5A mutant were linearized with PvuII. The template DNA truncated after the codon Asn⁹⁷ was transcribed by T7 RNA polymerase. Transcripts were translated in the rabbit reticulocyte lysate cell-free system at 25°C for 1 h. The translation mixture was layered on top of the 5% to 25% sucrose gradients and centrifuged for 1 h at 52,000 rpm in a S52-ST rotor (HITACHI). The gradient was fractionated into 20 fractions. The fractions were incubated with 1 mM SH-reactive homo-bi-functional crosslinker, BMOE at on ice for 1 h. The reactions were quenched by 100 mM DTT and proteins were precipitated with TCA, washed in acetone, analyzed by SDS-PAGE, and detected by autoradiography.

4.7. Immunofluorescence microscopy of full-length PMP70

COS7 cells expressing human PMP70-HA were fixed with 4% paraformaldehyde in PBS for 10 min, washed twice with PBS, and permeabilized with 0.2% Triton X-100 in PBS for 15 min. The fixed cells were incubated with PBS containing 1% BSA for 30 min and then incubated with mouse anti-HA monoclonal antibody and rabbit anti-Pex14 antiserum for 1 h. After

washing with PBS containing 0.1% Tween 20, cells were incubated with Alexa Fluor 488-conjugated anti-mouse IgG and Alexa Fluor 546-conjugated anti-rabbit IgG for 1 h. When coexpressed with EGFP-Cytb5, HA was visualized with mouse anti-HA monoclonal antibody and Alexa Fluor 546-conjugated anti-mouse IgG, and EGFP was visualized with anti-EGFP antibodies (21) and Alexa Fluor 488-conjugated anti-rabbit IgG. The cells were mounted with ProLong Antifade (Invitrogen) and observed using a laser scanning microscope.

5. Results

5.1. ER integration of TM1 is suppressed by an upstream 80-residue segment

As with other half-type isoforms of the ABC transporter family, PMP70 possesses six hydrophobic TM segments (3). In the upstream region of the TM1 segment, there is an 82-residue sequence that includes a weakly hydrophobic segment (termed H0 here) and a segment rich in positively-charged residues (Fig. 1A). I first investigated the ER-targeting properties of the TM1 and H0 segments using an *in vitro* system. The N-terminal segment of 111-residues of PMP70 (1-111) was fused to a mature prolactin domain with an artificial glycosylation site (PLg). When the PLg domain is fused to an appropriate signal sequence, it is translocated through the ER membrane and glycosylated in the lumen (30). The 1-111 construct contained two potential glycosylation sites; one is Asn¹⁰⁶ after the TM1 and the other is in the PLg domain. When synthesized in the reticulocyte lysate cell-free system in the absence of rough microsomal membrane (RM), a major 30-kDa product was observed (Fig. 1B, lane 1; closed circle). In the presence of RM, only a trace amount of a higher molecular-weight form was observed (Fig. 1B, lane 2; open triangle). The major band was degraded by externally added proteinase K (ProK), indicating that the PLg domain of the 1-111 construct was hardly translocated across the membrane.

To directly examine the function of the TM1 segment, the N-terminal portion (residues 2-79) was deleted (80-111; Fig. 1B). When synthesized in the presence of RM, the TM-segment was processed and both of the glycosylation sites were glycosylated (Fig. 1B and Fig. S1); a major processed diglycosylated form (closed square), minor split bands of monoglycosylated forms (open square), and a minor processed nonglycosylated form (open circle) were observed. Glycosylation was confirmed by Endoglycosidase H (EndoH) treatment (Fig. 1B lane 8). The two split bands of the monoglycosylated forms were most likely due to the mobility difference caused by the glycosylated positions. The monoglycosylated and diglycosylated forms were resistant to ProK, while the unprocessed-unglycosylated form was degraded (Fig. 1B, lane 7).

Signal peptide prediction and mutation analyses demonstrated that it was cleaved after the Cys⁹⁹ (Fig. S1). The glycosylation at Asn¹⁰⁶ occurred only when the TM1 segment was cleaved (Fig. S1 and Fig. 2). Positioning of signal peptidase cleavage sites is affected by the N-terminal domain flanking the TM1 and the length of the hydrophobic segment (31,32). The TM1 segment of the 80-111 construct induces efficient translocation of the downstream sequence and is processed by signal peptidase. These findings indicated that the TM1 segment possesses an intrinsic signal function and that the upstream 82-residue sequence suppresses ER-targeting.

I then examined the function of the N-terminal 40-residue segment including the H0-region. The 1-40 construct was neither glycosylated nor resistant to ProK, indicating that the H0-segment had no signal function (Fig. 1B, lanes 9-12).

5.2. N-terminal short motif suppresses the translocation by TM1 into the ER membrane

To determine the essential part within the N-terminal portion for suppressing ER targeting, various regions were deleted from the 1-111 fusion protein (Fig. 1C). The 60-111 protein yielded significantly larger glycosylated products (closed and open square) and processed smaller products (open circle), as observed with the 80-111 protein (Fig. 1C, lanes 4 and 6; Fig. S1). Although the precursor forms of the 60-111 and 80-111 proteins exhibited different mobilities, the processed and glycosylated forms exhibited the same mobilities (Fig. 1C, lanes 3-6). The smallest bands were likely processed forms and the largest bands were the diglycosylated forms of the processed molecules. Upon mutation of the predicted signal peptidase processing site (C99W), processing was silenced and diglycosylation was also greatly diminished (Fig. S1, lanes 8 and 17). Glycosylation at Asn¹⁰⁶ occurred only after the TM1 was processed.

When the N-terminal 9-residue sequence was deleted (10-111), the product yielded larger glycosylated form and smaller processed form (Fig. 1C, lane 8) by RM. The model proteins were partially processed and partially diglycosylated; the extent of processing and

glycosylation depended on the length of the N-terminal portion (for details, see Fig. S1). In any event, all of the smaller and larger forms indicated that the deletion constructs were inserted into the ER membrane. The N-terminal 9-residue sequence was essential for ER-targeting suppression. On the other hand, the $\Delta 19-80$ and $\Delta 10-79$ proteins yielded few glycosylated and no processed forms (Fig. 1C, lanes 10 and 12), indicating the N-terminal 9 residues are sufficient for ER-targeting suppression. When 4 (SKYL) or 2 (SK) residues within the 9 residues were deleted, the mutants were processed and glycosylated. These findings together clarify that the N-terminal 9-residue motif is essential for suppressing ER targeting and that Ser⁵ and Lys⁶ have key roles in this function.

5.3. Ser⁵ is essential for ER-targeting suppression

To determine the essential residues in the N-terminal segment, I performed alanine scanning (Fig. 2A). The S5A and K6A mutants caused efficient translocation of the PLg-domain. The other alanine substitutions had little effect. When the glycosylation site just after the TM1 was silenced (Fig. 2B, T108A), the larger processed form (closed square) was not observed and the unprocessed-glycosylated form (open triangle) was not affected, indicating that the larger unprocessed form (open triangle) was not glycosylated at Asn¹⁰⁶ and that the larger processed form (closed square) was glycosylated both at Asn¹⁰⁶ and the PLg-domain site. The signal-peptidase processing site (Cys⁹⁹-Asp¹⁰⁰) was predicted using a SignalP prediction algorithm. When the processing site was silenced by a point mutation (C99W), the smaller products were no longer observed and only the unprocessed-monoglycosylated form was observed (compare Fig. 2B lanes 2 and 8). Products smaller than the precursor form were generated by processing at Cys⁹⁹. Treatment with ProK (Fig. S2A) demonstrated that the TM1 of the S5A mutant of 1-111 residues spans the membrane (Fig. 2B). The processing and glycosylation both are definitive indications of ER insertion of the TM1 segment. The ER integration percent was estimated by quantifying the processed forms and the

unprocessed-monoglycosylated forms among the total products (Fig. 2B, lower panel). All the above data demonstrated that a single amino acid substitution (S5A or K6A) of the 1-111 construct led to efficient ER membrane insertion.

To examine the importance of the Ser⁵ residue, it was exchanged with the other 19 amino acids (Fig. 2C). All the mutants yielded a large amount of the unprocessed-monoglycosylated and the processed glycosylated forms. The percent of the unprocessed-monoglycosylated form (band b) and the processed-diglycosylated form (band c) among the synthesized polypeptide chains showed efficient targeting of the mutants to the ER. Very minor changes (e.g., Ser to Thr and Ser to Ala) resulted in efficient ER targeting, indicating the absolute importance of the Ser⁵ residue for suppressing ER integration. When the Lys⁶ was mutated (Fig. 2D), Arg could functionally replace the Lys residue and Val could partially replace its function, suggesting that a bulky residue could replace the function of Lys⁶. The specific requirement of Ser⁵ strongly suggests that a specific recognition of the motif is involved in the ER-targeting suppression.

5.4. Importance of the N-terminal region was confirmed in the cells

I then examined the function of the N-terminal region of PMP70 in cultured cells (Fig. 3). The 1-111 protein and its mutant constructs were transiently expressed in COS7 cells. In these experiments, I carefully estimated the minimum amount of plasmid required to detect the products by immunoblotting. The wild-type and mutants gave different results. Only a trace amount of products of the wild-type 1-111 fusion protein could be detected (Fig. 3A, lane 1). On the other hand, strong smaller molecular weight bands were detected with the S5A and K6D mutants (Fig. 3A, lanes 3 and 5, closed squares). Those forms possessed an EndoH-sensitive sugar chain and were fully resistant against ProK treatment (Fig. S2B), indicating that they were processed-glycosylated forms in the ER lumen. When they were expressed in the presence of the proteasome inhibitor MG132, a product of the wild-type construct was newly observed

(Fig 3A, closed circle). It was sensitive to ProK and not affected by EndoH treatment (Fig. S1B), indicating that this was the unprocessed-nonglycosylated form. With the mutated constructs, the unprocessed-nonglycosylated form and unprocessed-monoglycosylated form were newly observed (closed circles and open triangles). The glycosylation was confirmed by EndoH treatment (Fig. S2B). The majority of the wild-type 1-111 fusion protein was not targeted to the ER. The unprocessed-nonglycosylated form remained in the cytosol and was rapidly degraded by proteasomes. In contrast, the point mutants (S5A and K6D) were largely targeted to the ER, processed and glycosylated as observed in the cell-free system. The processed-diglycosylated forms were stable even in the absence of MG132. The C99W mutation inhibited processing, as observed in the cell-free system (Fig. 3A, lane 8), confirming processing at the Cys⁹⁹ by the signal peptidase in the cells. The processing of the (S5A)1-111 construct in the cells was more efficient than in the cell-free system for an unknown reason. Wild-type 1-111 fusion protein was hardly integrated into the ER and was rapidly degraded by proteasomes, whereas the S5A and K6D mutants were ER-targeted and stably observed. These results indicated that the N-terminal region suppressed ER-targeting in the cell as well, and that Ser⁵ and Lys⁶ were critical for the function.

5.5. A short motif can suppress the signal peptide function of pre-prolactin

To examine whether the motif suppresses the authentic signal peptide, the N-terminal 12-residue sequence (N12) was fused to the N-terminus of pre-prolactin (pPL; Fig. 4A, N12-pPL). When synthesized in the absence of RM, the precursor form of pPL was observed (Fig. 4B). When synthesized in the presence of various amounts of RM, pPL was processed to the mature form depending on the amount of RM. In the case of N12-pPL, the processing was greatly suppressed. In contrast to the drastic effect of N12, its S5A mutant was processed as efficiently as the original pPL.

The fusion proteins were also examined in COS7 cells (Fig. 4C). When pPL was

transiently expressed for 24 h, only the mature form of prolactin was detected. In the case of pPL and (S5A)N12-pPL, only the processed mature form of prolactin was observed. When expressed in the presence of MG132, the amounts increased. The mature form of prolactin was fully resistant to ProK, indicating pPL and (S5A)N12-pPL were translocated into the ER membrane. In contrast, only the precursor form of N12-pPL was observed in the presence of MG132. ProK degraded the precursor form, indicating the presence of N12-pPL in the cytoplasm. Thus, N12 suppressed the function of the prolactin signal peptide in the cells and Ser⁵ was essential for the suppression.

5.6. N12 is effective only at the N-terminus of the nascent chain

To address the effect of the positioning, glycine residue was serially added to the N-terminus of the motif (Fig. 5). The constructs were assessed in the wheat germ extract cell-free system in addition to the reticulocyte lysate system in the presence of increasing amounts of RM. The N12-sequence suppressed the signal peptide function of pPL in both translation systems. While the addition of one glycine had little effect on the ER-targeting suppression, insertion of two glycines largely inhibited the targeting suppression and insertion of three glycines caused a complete loss of function. The ER-targeting suppression function of the motif was also confirmed in a plant cell-free system. It should be at the N-terminus for proper function.

5.7. N12 function was competitively inhibited by N12-fusion protein

To address the possibility that some N-motif binding factors are involved in the ER targeting suppression, I examined the effect of the fusion protein of the N12-motif and glutathione-S-transferase (Fig. 6). The fusion protein and the S5A mutant were expressed in *E. coli* and purified. The processing and glycosylation of the 1-111 construct was enhanced by the N12-GST fusion protein, depending on the amounts (Fig. 6B). The S5A-mutated fusion protein had no effect. Processing of the N12-pPL was also enhanced in a dose-dependent manner, while

the S5A mutant fusion protein showed no effect (Fig. 6C). I performed similar experiments with a synthetic peptide of the N-motif and obtained essentially the same results (data not shown). Suppression of ER targeting was competitively abrogated by GST-fusion proteins, strongly suggesting that saturable factors are involved in the ER-targeting suppression mechanism.

5.8. The 50-kDa and the 20-kDa factors were crosslinked with the N12-nascent chains

To probe cytosolic factors involved in ER-targeting suppression, I performed crosslinking experiments. The ER-targeting of secretory proteins or membrane proteins occurs cotranslationally, and therefore I considered that putative factors should bind the N12-nascent chain elongating from the ribosome. Ribosome nascent chain complexes (RNCs) of N12-pPL or the S5A mutant were generated in the cell-free system using mRNAs truncated after the pPL codon 97 (Fig. 7A). The amino acid sequence of the RNC includes three cysteines (Cys³⁶, Cys⁴⁵, and Cys⁵²) and the signal peptide of prolactin is exposed outside the ribosome. When the RNCs in the translation mixture were directly subjected to chemical crosslinking with bismaleimidoethane (BMOE), I detected no crosslinked products (data not shown) because bulk proteins in the reticulocyte lysate inhibited the reactions. To remove the large amount of proteins in the cell-free translation system, I fractionated the reticulocyte lysate by sucrose density gradient centrifugation before the crosslinking reaction. I detected specific crosslinked products with the N12 nascent chain (Fig. 7B). The RNCs of the N12-pPL generated two specific crosslinked products (arrows) in addition to nonspecific products that were also detected with the S5A mutant (open circles). Considering the molecular mass of the N12-pPL 97RNC (~10 kDa), the specific crosslinking proteins were likely ~50 kDa and ~20 kDa. These findings suggest the existence of the protein factors that recognize the RNCs of the N-motif during the cotranslational ER-targeting.

5.9. S5A mutation caused mislocation of PMP70 to the ER in cultured cells

I examined the importance of Ser⁵ for the subcellular localization of full-length PMP70. PMP70 C-terminally fused to the HA-tag was transiently expressed in COS7 cells in the presence or absence of MG132 and detected by immunoblotting (Fig. 8A). Wild-type PMP70 was detected regardless of the presence or absence of MG132, while the S5A mutant was only detected in the presence of MG132. Immunofluorescence microscopy observation revealed that regardless of the presence or absence of MG132, wild-type PMP70-HA expressed in COS7 cells located in a punctate structure and co-localized with endogenous Pex14, the peroxisomal marker (Fig. 8B right). In the absence of MG132, the S5A mutant was expressed in a few cells and located in peroxisomal structures. On the other hand, in the presence of MG132, the numbers of cells expressing the S5A mutant increased and the mutant was localized in the reticular structure of the ER (Fig. 8B left). When coexpressed with the ER marker protein (EGFP-Cytb5) (20), the reticular structure of the S5A mutant was well costained (Fig. 8C). These results indicated that the S5A mutant of PMP70 mislocalized to the ER and was degraded by the proteasome. Ser⁵ of PMP70 is essential for correct targeting to the peroxisome.

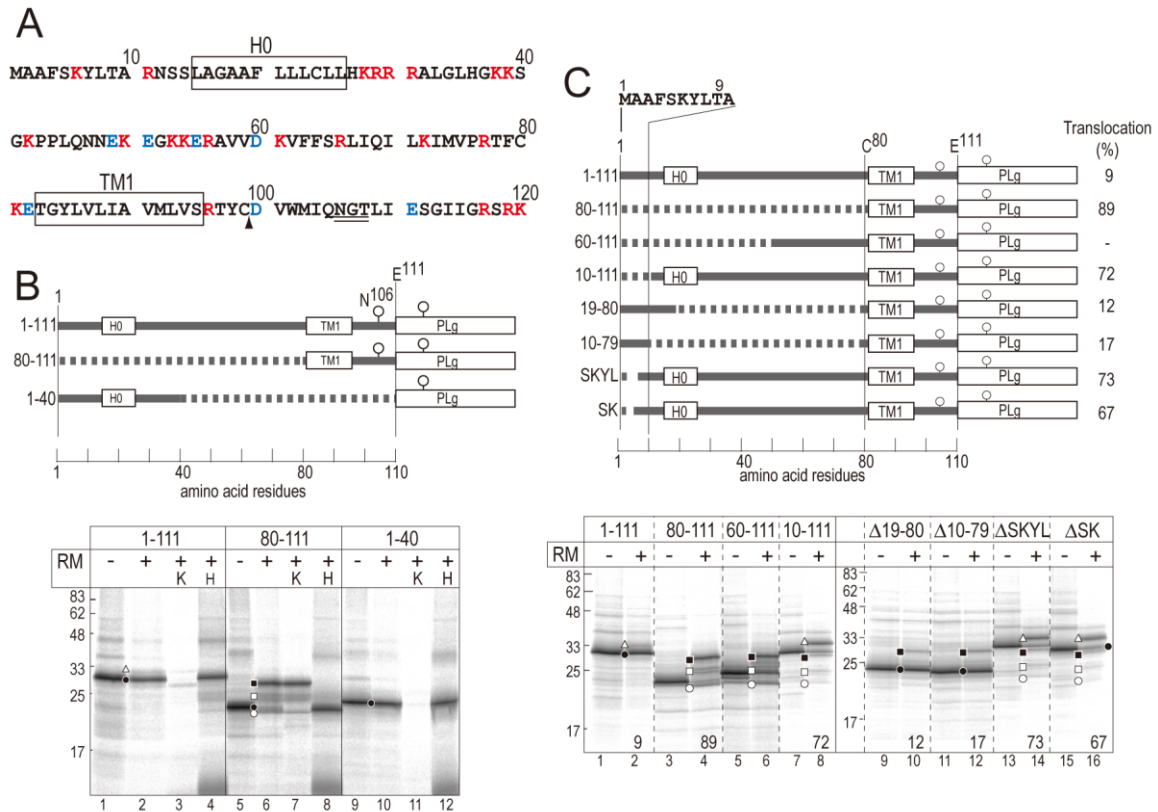


Figure 1. An N-terminal short motif suppresses ER integration of TM1.

(A) N-terminal sequence of PMP70. Hydrophobic segments (H0 and TM1) are boxed. Basic amino acids (red), acidic amino acids (blue), the endogenous glycosylation site (Asn¹⁰⁶, double underline), and the anticipated processing site (arrowhead) are indicated. (B) The N-terminal portions (Met¹-Glu¹¹¹, Cys⁸⁰-Glu¹¹¹, and Met¹-Ser⁴⁰) were fused to the reporter domain of PLg. Potential glycosylation sites (open circles) are indicated. The fusion proteins were expressed in a cell-free system in the presence and absence of RM (RM + and – lanes, respectively). Aliquots of the translation products were treated with ProK and EndoH (K and H lanes, respectively). Symbols indicate the processed-diglycosylated form (closed square), the processed-monoglycosylated form (open square), the unprocessed-unglycosylated form (closed circle), the processed-unglycosylated form (open circle), and unprocessed-monoglycosylated form (open triangle). (C) Various portions of the 1-111 fusion protein (dotted lines) were deleted. Numbers indicate residue numbers of mouse PMP70. The rectangle indicating the PLg reporter domain is not to scale. The constructs were expressed in

the absence or presence of RM. The percent of PLg domain translocation was estimated as the percent of processed and/or glycosylated forms among the total products (for detail see Materials and methods). In the case of 60-111, the percent was not determined, as the precursor form and the processed monoglycosylated form exhibited the same mobility on the gel and could not be separately quantified. The Δ SK construct was partially processed. The processing and glycosylation status, and membrane topology of the fusion proteins are demonstrated in Figures S1 and S2.

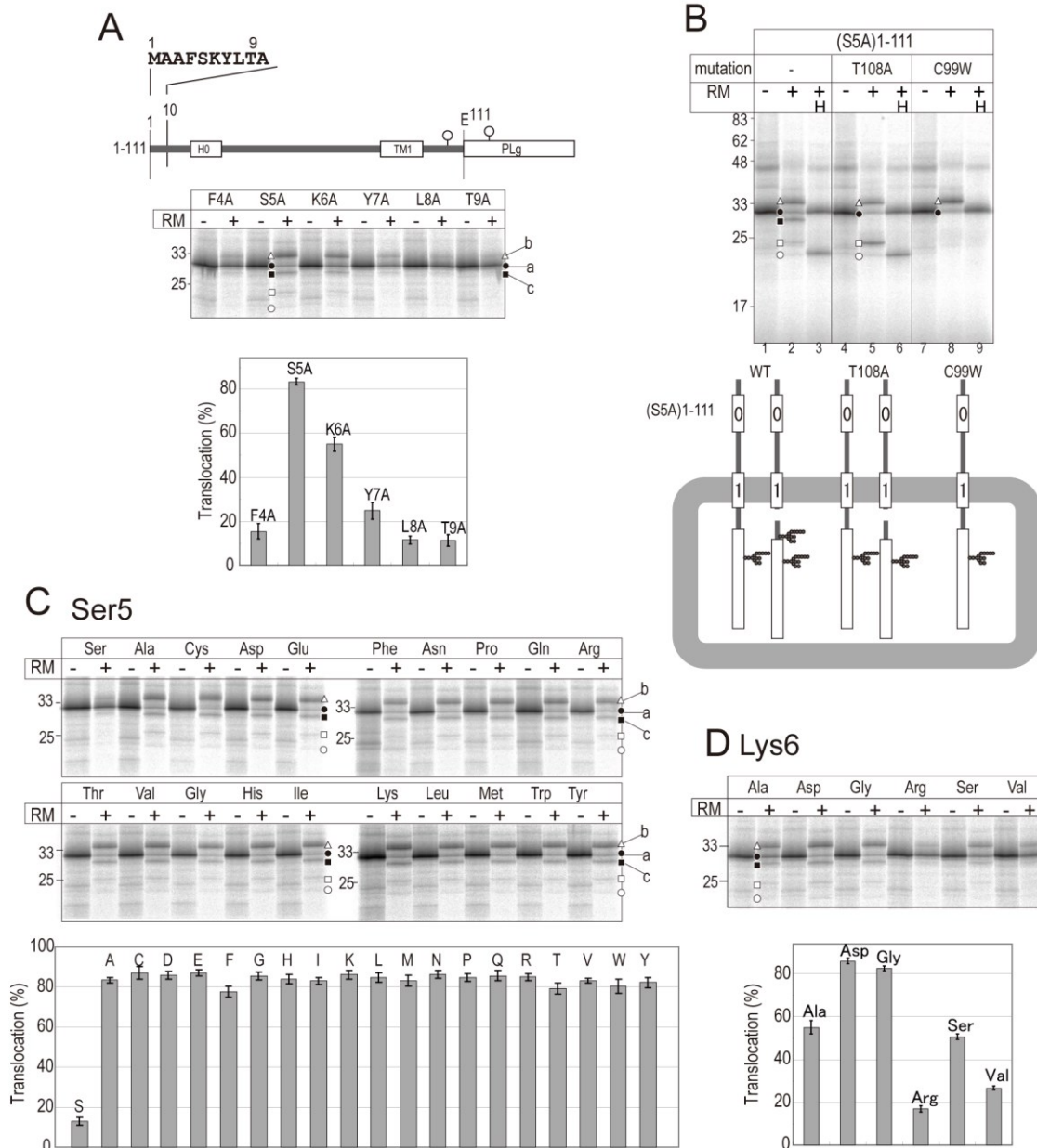


Figure 2. Ser⁵ and Lys⁶ are essential for ER-targeting suppression.

(A) Alanine scanning of the N-terminal region was performed using the 1-111 construct. Each residue was exchanged with Ala and the mutants were expressed in a cell-free system. The mean values of membrane translocation and SD are indicated. (B) Glycosylation and processing of the (S5A)1-111 construct was examined. Each mutant was translated *in vitro* and the aliquot was treated with EndoH. The T108A mutation silenced glycosylation at Asn¹⁰⁶. The C99W mutation inhibited the processing after the TM1 segment. Schema represents membrane topology and glycosylation status. Asn¹⁰⁶ is glycosylated only when the TM1 is cleaved off.

One half of the (S5A)1-111 construct was processed and the former potential site (Asn¹⁰⁶) became accessible to oligosaccharyltransferase. The unprocessed form was hardly glycosylated at Asn¹⁰⁶. (C and D) The critical Ser and Lys residues were exchanged with the indicated residues. The mean translocation percent of the PLg-domain is indicated with SDs.

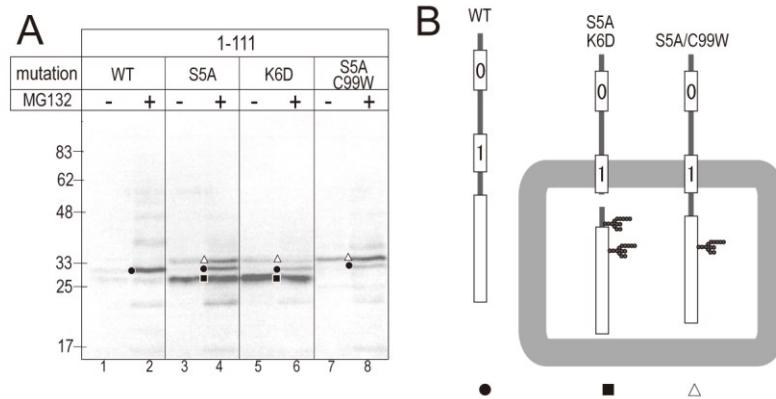


Figure 3. Requirements of Ser⁵ and Lys⁶ demonstrated in living cells.

(A) The 1-111 construct and its mutants were transiently expressed in COS7 cells. Where indicated, MG132 was included for 9 h before sampling. Cells were directly subjected to SDS-PAGE and the prolactin domain was detected by immunoblotting. The unprocessed-nonglycosylated form (closed circle), processed-diglycosylated form (closed square), and unprocessed-monoglycosylated form (open triangle) are indicated. (B) Membrane topology of the products. The S5A and K6A mutations caused targeting and translocation of the PLg domain. The wild-type 1-111 construct is rarely integrated in the ER membrane (closed circle) and detected only in the presence of the proteasome inhibitor MG132.

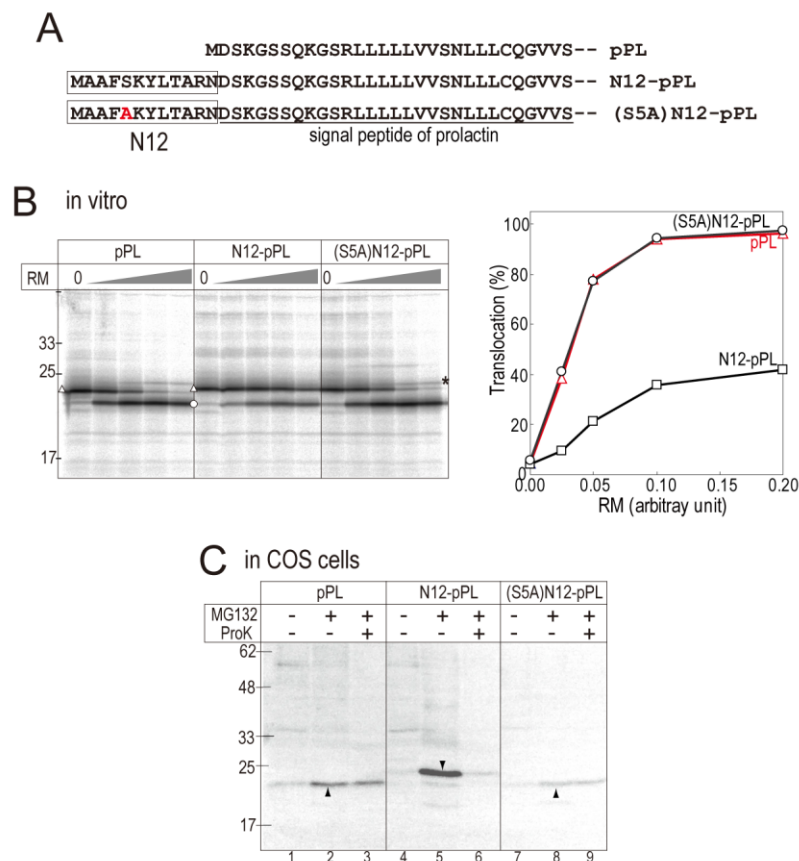


Figure 4. N-terminal 12-residue motif suppresses prolactin signal peptide.

(A) The N-terminal 12-residue segment of PMP70 (N12) and its S5A mutant were fused to the N-terminus of pPL (without a glycosylation site). (B) ER translocation was assessed *in vitro* (left panel). The amount of RM was titrated as indicated in the right panel. The precursor form (open triangle) and processed form (open circle) are indicated. Trace amounts of the polypeptide glycosylated at the noncanonical site (at Cys⁹⁷) are indicated (asterisk). Processing percentage (%) was determined (right panel). (C) The fusion proteins were transiently expressed in COS7 cells for 24 h. Where indicated, MG132 was included for 9 h before sampling. Cells were permeabilized with a low concentration of digitonin (25 μ g/ml) in culture dishes and aliquots were treated with ProK. Cells were subjected to SDS-PAGE and the prolactin domain was detected by immunoblotting. The precursor form (downward arrowhead) and the processed mature form (upward arrowhead) are indicated.

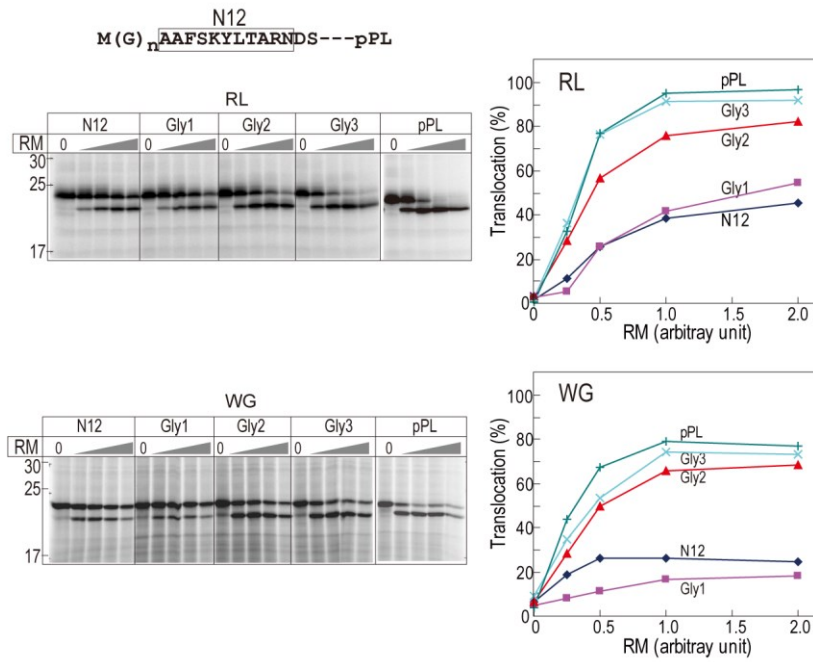


Figure 5. Effect of N-terminal extension on the N12-motif function

Glycine residues were inserted after the initiation methionine of the N12-pPL construct. The mutants were translated in reticulocyte lysate and wheat germ extract cell-free systems. The amount of RM was titrated as indicated in the right panels. Processing efficiency (%) was quantified and plotted in the right panel.

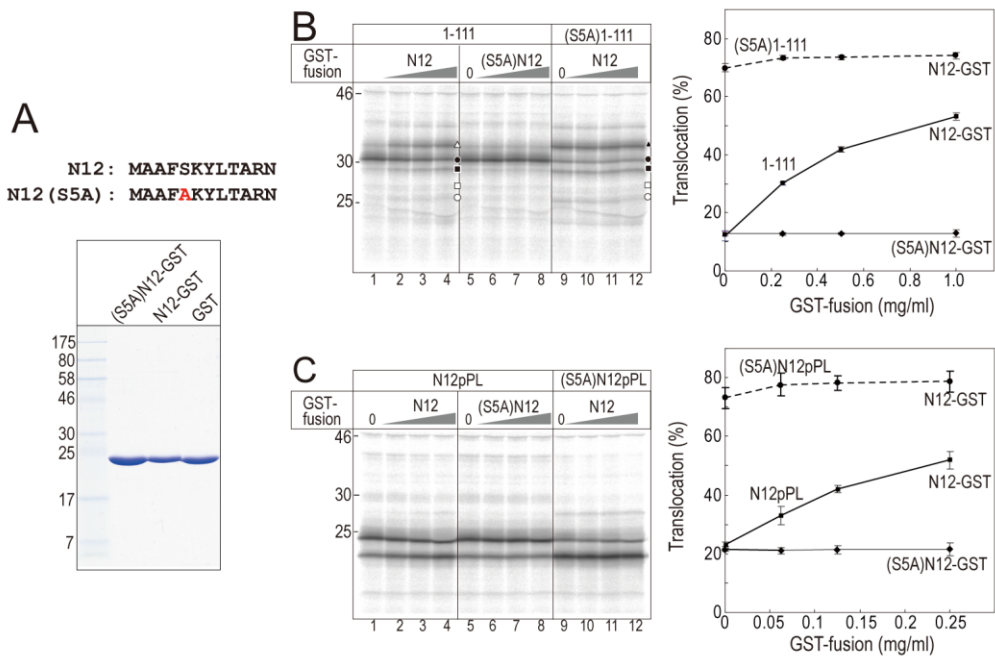


Figure 6. Effect of N12-GST fusion protein on the N12-motif function

(A) N12-GST fusion protein and its S5A mutant were expressed in *E. coli* and purified. Purified proteins (5 μ g each) were analyzed with SDS-PAGE and visualized by Coomassie Brilliant Blue stain. (B) Effect on translocation of the 1-111 construct. The 1-111 construct and its S5A mutant were translated in a reticulocyte cell-free system supplemented with RM, in the presence of N12-GST and its S5A mutant fusion proteins. Symbols are the same as in Figure 2. The translocation percentage was quantified as in Figure 2 and the mean and SD values are shown in the right panel. (C) Effect of the fusion proteins on N12-pPL translocation.

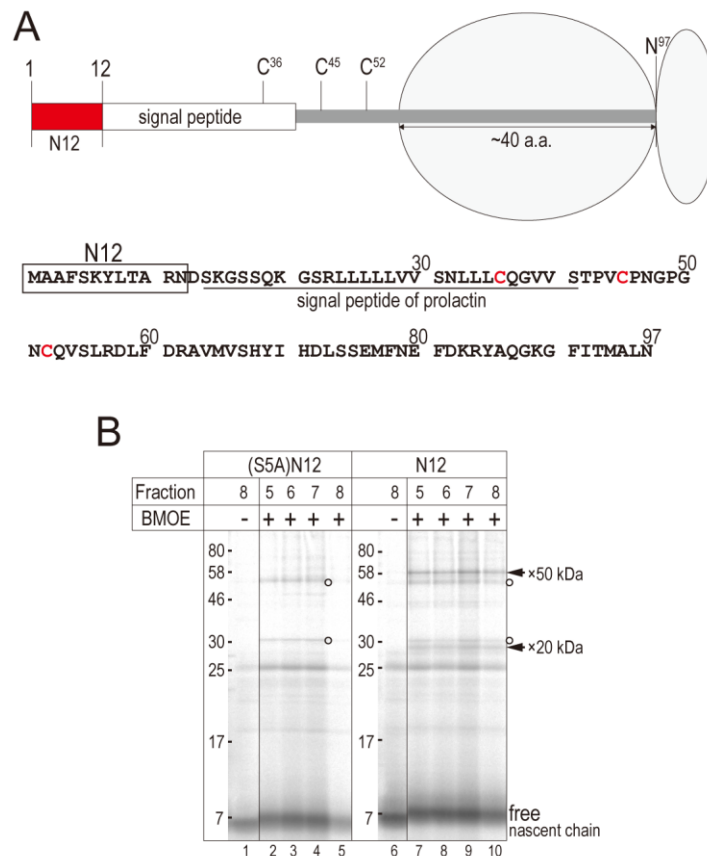


Figure 7. Two protein factors are crosslinked with the N12-nascent chain

(A) RNAs encoding the N12-pPL and its S5A mutant were truncated at Asn⁹⁷, and translated *in vitro* to generate the ribosome nascent chain complex. Considering that the length of the ribosomal tunnel is ~40 residues, the signal peptide of prolactin is exposed outside of the ribosome. The sequence of the nascent chain, the N12 sequence (box), cysteine residue (red), and the signal peptide of prolactin (underline) are indicated. (B) Translation reactions were fractionated by sucrose density gradient centrifugation and subjected to a crosslinking reaction with BMOE. The lowest bands represent the free nascent chain (~10 kDa). Although some proteins are crosslinked with both N12 and the S5A nascent chain (open circle), two proteins (~50 kDa and ~20 kDa, arrow) were specifically crosslinked with the N12-nascent chain.

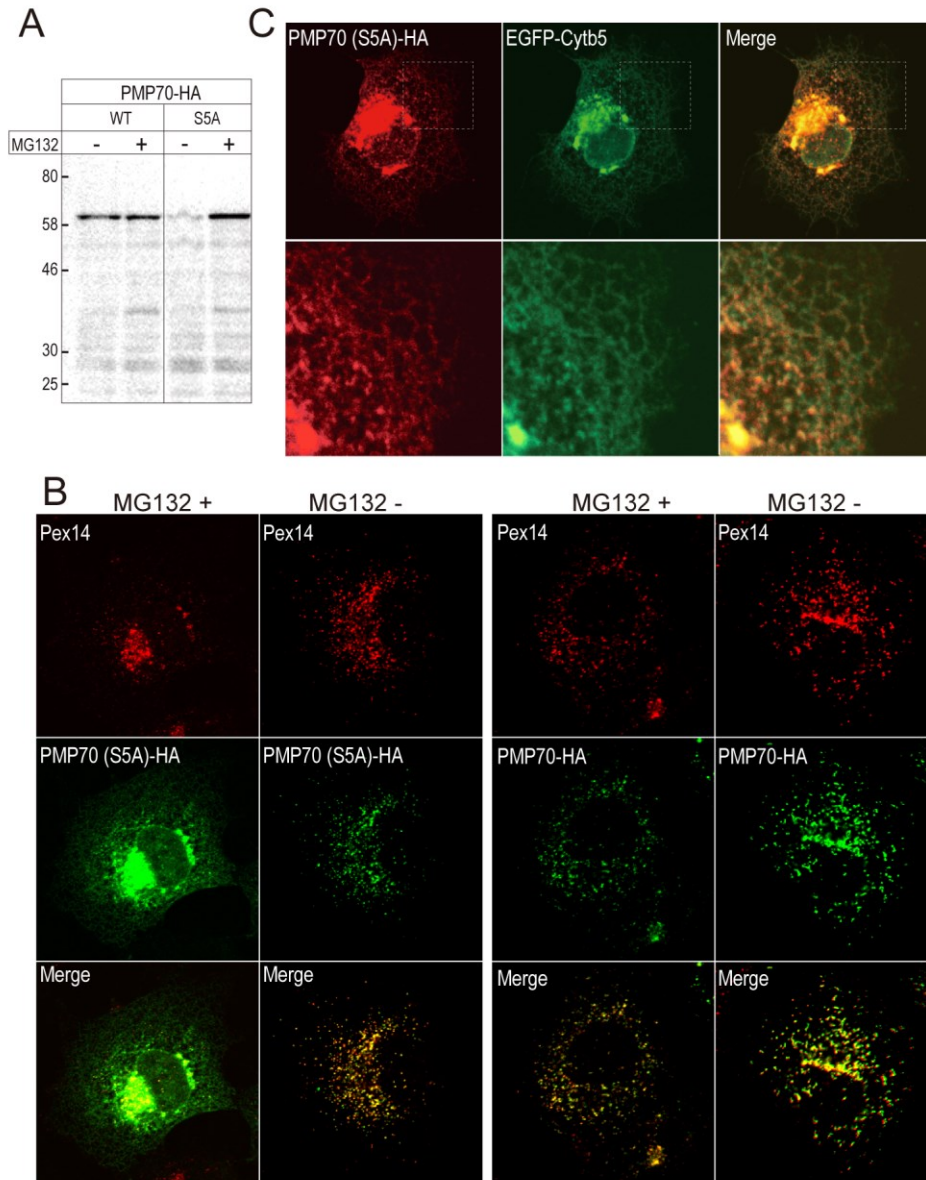


Figure 8. Point mutation S5A caused mislocalization of PMP70 to the ER.

(A) PMP70-HA and (S5A)PMP70-HA were transiently expressed in COS7 cells. Cells were incubated in the presence or absence of MG132 for 12 h before sampling. Expression of the PMP70 molecules was monitored by SDS-PAGE and subsequent immunoblotting. (B) Cells expressing PMP70-HA or the S5A mutant were immunostained and observed by fluorescence microscopy. Endogenous Pex14 was used as the peroxisomal marker. (C) PMP70(S5A)-HA was coexpressed with EGFP-Cytb5 (marker of ER) and the expressed EGFP fusion was immunostained with anti-EGFP antibodies. The area indicated by dashed box is magnified below.

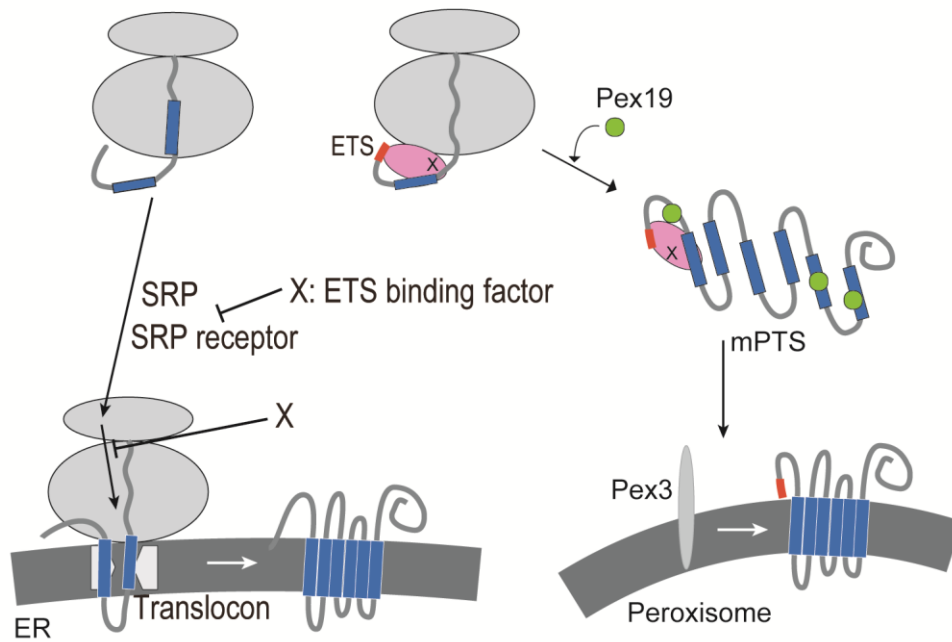


Figure 9. Working model of ETS function.

In the presence of ETS on the PMP70 nascent chain, ETS is recognized by ETS binding factors at the exit of the ribosome and the cotranslational targeting by the following TM segment is suppressed. ETS and the binding factors may suppress the function of signal recognition particle (SRP) and its receptor. Alternatively, they may suppress the recognition by translocon. Pex19 binds multiple sites of the PMP70 nascent chain and keeps it soluble. And then the fully-elongated nascent chain is targeted to peroxisome by Pex3 and membrane protein peroxisome targeting signal (mPTS). In the absence of ETS, TM segment is targeted to ER translocon. The PMP70 molecule is likely unstable on the ER and rapidly degraded by proteasomes.

6. Discussion

Here I examined the ER targeting characteristics of the N-terminal portion of PMP70 and found that the TM1 segment possesses strong ER targeting function. The ER targeting was suppressed by the N-terminal short motif. Some saturable factors are most likely involved in this unique function. Based on my findings, I propose the concept of an "ER targeting suppressor (ETS)" as one of topogenic signal sequences in the cell. The ETS prevents cotranslational ER targeting of the hydrophobic signal sequences and allows them to be inserted into membrane organelles outside the secretory pathway.

Short sequence of less than 10 residues of PMP70 is sufficient for the ETS function. The motif can suppress the ER targeting of the other signal peptide of the unrelated secretory protein. Among these amino acid residues, Ser⁵ was indispensable for the ETS function and Lys⁶ was required for full-function. The N-terminal location of the motif was essential for the ETS function. The ETS functions on the PMP70 TM1 segment and on the pPL signal peptide were demonstrated not only in cell-free systems, but also in living cells.

Hydrophobic sequences always tend to be targeted to the ER translocon as the ER targeting signal. In some contexts, hydrophobic sequences stop translocation at the translocon and are released into the hydrophobic environment as a TM segment. Various sequence motifs for localization in the secretory pathway and various organelle-targeting signals have been elucidated. Positive charges of the nascent chain play critical functions as topogenic elements during membrane integration; they arrest movement in the translocon channel, determine the orientation of the hydrophobic signal sequence at the translocon, and stabilize the TM segment on the membrane. In addition to these topogenic units, the ETS is a critical unit. It prevents ER targeting of hydrophobic segments and allows hydrophobic membrane proteins to target organelles outside of the secretory pathway (Fig. 9).

The competition experiment decisively demonstrated that a saturable factor is involved in the ETS mechanism. Affinity purification using N12-GST protein has not yet been

successful, however, suggesting that the affinity is not sufficient. The affinities observed with organelle-targeting signals and the receptors are generally moderate; e.g., the dissociation constant between the mitochondrial presequence and its primary receptor Tom20 is reported to be 8×10^{-6} M (33). Specific binding factors, however, were detected by chemical crosslinking with the N12-nascent chain ribosome complex. Those 50-kDa and 20-kDa proteins are the postulated factors. Crosslinking with N12-RNC as an assay procedure allows the postulated proteins to be fractionated by ammonium sulfate precipitation and several column chromatography steps (data not shown). The proteins could then be identified, and cell-biologic examination of the factors would provide key information regarding the mechanism involved in the sorting of PMPs.

The S5A mutation caused the full-length PMP70 molecule to localize in the ER. In the simple transient transfection experiment, the HA-tagged wild-type PMP70 clearly localized in the punctate structures in the absence of MG132, indicating they normally localize in the peroxisome. Upon the Ser5Ala mutation, cells expressing the PMP70 molecule dramatically decreased in the absence of MG132 compared with the wild-type transfection experiment. In the presence of the proteasome inhibitor, the cell numbers expressing mutant PMP70-HA molecules appeared to increase at least 5 times (data not shown), and the amount of the expressed protein clearly increased (Fig. 8A). Under these conditions, the mutant molecules were observed dominantly in the reticular organelle of the ER. The mutation (Ser5Ala) inactivated the ETS and led to ER targeting. The ER-targeted molecules were rapidly degraded by the proteasome system. In some cells, the mutant molecules were overexpressed and small portions located in the peroxisomes independently of the ETS, where even the mutant PMP70 should be stable.

Many peroxisomal membrane proteins have been suggested to be inserted into the ER membrane and then sorted to peroxisomes (34)). The existence of the ETS as a functional unit in the nascent chain strongly suggests that a group of peroxisomal membrane proteins would

obligatorily escape the ER and be directly targeted to the peroxisomes. At least, the TM1 segment cannot be cotranslationally inserted into the ER membrane in the presence of the ETS. Clarification of ETS function and the recognition factors would lead to a better understanding of the pleiotropic regulation of membrane protein sorting.

7. References

1. Egea, P. F., Stroud, R. M., and Walter, P. (2005) Targeting proteins to membranes: structure of the signal recognition particle. *Curr. Opin. Struct. Biol.* **15**, 213-220
2. Rapoport, T. A. (2007) Protein translocation across the eukaryotic endoplasmic reticulum and bacterial plasma membranes. *Nature* **450**, 663-669
3. Tusnády, G. E., Sarkadi, B., Simon, I., and Váradi, A. (2006) Membrane topology of human ABC proteins. *FEBS Lett.* **580**, 1017-1022
4. Miyazaki, E., Kida, Y., Mihara, K., and Sakaguchi, M. (2005) Switching the sorting mode of membrane proteins from cotranslational endoplasmic reticulum targeting to posttranslational mitochondrial import. *Mol. Biol. Cell.* **16**, 1788-1799
5. Graf, S. A., Haigh, S. E., Corson, E. D., and Shirihai, O. S. (2004) Targeting, import, and dimerization of a mammalian mitochondrial ATP binding cassette (ABC) transporter, ABCB10 (ABC-me). *J. Biol. Chem.* **279**, 42954-42963
6. Honsho, M., and Fujiki, Y. (2001) Topogenesis of peroxisomal membrane protein requires a short, positively charged intervening-loop sequence and flanking hydrophobic segments. study using human membrane protein PMP34. *J. Biol. Chem.* **276**, 9375-9382
7. Jones, J. M., Morrell, J. C., and Gould, S. J. (2001) Multiple distinct targeting signals in integral peroxisomal membrane proteins. *J. Cell Biol.* **153**, 1141-1150
8. Fujiki, Y., Okumoto, K., Mukai, S., Honsho, M., and Tamura, S. (2014) Peroxisome biogenesis in mammalian cells. *Front. Physiol.* **5**, 307
9. Kikuchi, M., Hatano, N., Yokota, S., Shimozawa, N., Imanaka, T., and Taniguchi, H. (2004) Proteomic analysis of rat liver peroxisome: presence of peroxisome-specific isozyme of Lon protease. *J. Biol. Chem.* **279**, 421-428
10. Kashiwayama, Y., Asahina, K., Morita, M., and Imanaka, T. (2007) Hydrophobic regions adjacent to transmembrane domains 1 and 5 are important for the targeting of

- the 70-kDa peroxisomal membrane protein. *J. Biol. Chem.* **282**, 33831-33844
11. Rottensteiner, H., Kramer, A., Lorenzen, S., Stein, K., Landgraf, C., Volkmer-Engert, R., and Erdmann, R. (2004) Peroxisomal membrane proteins contain common Pex19p-binding sites that are an integral part of their targeting signals. *Mol. Biol. Cell* **15**, 3406-3417
 12. Fransen, M., Wylin, T., Brees, C., Mannaerts, G. P., and Van Veldhoven, P. P. (2001) Human pex19p binds peroxisomal integral membrane proteins at regions distinct from their sorting sequences. *Mol. Cell Biol.* **21**, 4413-4424
 13. Halbach, A., Lorenzen, S., Landgraf, C., Volkmer-Engert, R., Erdmann, R., and Rottensteiner, H. (2005) Function of the PEX19-binding site of human adrenoleukodystrophy protein as targeting motif in man and yeast. PMP targeting is evolutionarily conserved. *J. Biol. Chem.* **280**, 21176-21182
 14. Sacksteder, K. A., Jones, J. M., South, S. T., Li, X., Liu, Y., and Gould, S. J. (2000) PEX19 binds multiple peroxisomal membrane proteins, is predominantly cytoplasmic, and is required for peroxisome membrane synthesis. *J. Cell Biol.* **148**, 931-944
 15. Kashiwayama, Y., Asahina, K., Shibata, H., Morita, M., Muntau, A. C., Roscher, A. A., Wanders, R. J., Shimozawa, N., Sakaguchi, M., Kato, H., and Imanaka, T. (2005) Role of Pex19p in the Targeting of PMP70 to Peroxisome. *Biochim. Biophys. Acta* **1746**, 116-128
 16. Kinoshita, N., Ghaedi, K., Shimozawa, N., Wanders, R. J., Matsuzono, Y., Imanaka, T., Okumoto, K., Suzuki, Y., Kondo, N., and Fujiki, Y. (1998) Newly identified Chinese hamster ovary cell mutants are defective in biogenesis of peroxisomal membrane vesicles (Peroxisomal ghosts), representing a novel complementation group in mammals. *J. Biol. Chem.* **273**, 24122-24130
 17. Iwashita, S., Tsuchida, M., Tsukuda, M., Yamashita, Y., Emi, Y., Kida, Y., Komori, M., Kashiwayama, Y., Imanaka, T., and Sakaguchi, M. (2010) Multiple organelle-targeting

- signals in the N-terminal portion of peroxisomal membrane protein PMP70. *J. Biochem.* **147**, 581-590
18. Walter, P., and Blobel, G. (1983) Preparation of microsomal membranes for co-translational protein translocation. *Methods Enzymol.* **96**, 84-93
 19. Jackson, R. J., and Hunt, T. (1983) Preparation and use of nuclease-treated rabbit reticulocyte lysates for the translation of eukaryotic messenger RNA. *Methods Enzymol.* **96**, 50-74
 20. Tsuchida, M., Emi, Y., Kida, Y., and Sakaguchi, M. (2008) Human ABC transporter isoform B6 (ABCB6) localizes primarily in the Golgi apparatus. *Biochem. Biophys. Res. Commun.* **369**, 369-375
 21. Miyazaki, E., Sakaguchi, M., Wakabayashi, S., Shigekawa, M., and Mihara, K. (2001) NHE6 protein possesses a signal peptide destined for endoplasmic reticulum membrane and localizes in secretory organelles of the cell. *J. Biol. Chem.* **276**, 49221-49227
 22. Siegel, V., and Walter, P. (1988) Each of the activities of signal recognition particle (SRP) is contained within a distinct domain: analysis of biochemical mutants of SRP. *Cell* **52**, 39-49
 23. Weiner, M. P., Costa, G. L., Schoettlin, W., Cline, J., Mathur, E., and Bauer, J. C. (1994) Site-directed mutagenesis of double-stranded DNA by the polymerase chain reaction. *Gene* **151**, 119-123
 24. Nielsen, H., Engelbrecht, J., Brunak, S., and von Heijne, G. (1997) Identification of prokaryotic and eukaryotic signal peptides and prediction of their cleavage sites. *Protein Eng.* **10**, 1-6
 25. Kanki, T., Sakaguchi, M., Kitamura, A., Sato, T., Mihara, K., and Hamasaki, N. (2002) The tenth membrane region of band 3 is initially exposed to the luminal side of the endoplasmic reticulum and then integrated into a partially folded band 3 intermediate. *Biochemistry* **41**, 13973-13981

26. Sakaguchi, M., Hachiya, N., Mihara, K., and Omura, T. (1992) Mitochondrial porin can be translocated across both endoplasmic reticulum and mitochondrial membranes. *J. Biochem.* **112**, 243-248
27. Kida, Y., Mihara, K., and Sakaguchi, M. (2005) Translocation of a long amino-terminal domain through ER membrane by following signal-anchor sequence. *EMBO J.* **24**, 3202-3213
28. Deprez, P., Gautschi, M., and Helenius, A. (2005) More than one glycan is needed for ER glucosidase II to allow entry of glycoproteins into the calnexin/calreticulin cycle. *Mol. Cell* **19**, 183-195
29. Kanaji, S., Iwahashi, J., Kida, Y., Sakaguchi, M., and Mihara, K. (2000) Characterization of the signal that directs Tom20 to the mitochondrial outer membrane. *J. Cell Biol.* **151**, 277-288
30. Ota, K., Sakaguchi, M., Hamasaki, N., and Mihara, K. (1998) Assessment of topogenic functions of anticipated transmembrane segments of human band 3. *J. Biol. Chem.* **273**, 28286-28291
31. Nilsson, I., Whitley, P., and von Heijne, G. (1994) The COOH-terminal ends of internal signal and signal-anchor sequences are positioned differently in the ER translocase. *J. Cell Biol.* **126**, 1127-1132
32. Haeuptle, M. T., Flint, N., Gough, N. M., and Dobberstein, B. (1989) A tripartite structure of the signals that determine protein insertion into the endoplasmic reticulum membrane. *J. Cell Biol.* **108**, 1227-1236
33. Schleiff, E., and Turnbull, J. L. (1998) Characterization of the N-terminal targeting signal binding domain of the mitochondrial outer membrane receptor, Tom20. *Biochemistry* **37**, 13052-13058
34. Dimitrov, L., Lam, S. K., and Schekman, R. (2013) The role of the endoplasmic reticulum in peroxisome biogenesis. *Cold Spring Harb. Perspect. Biol.* **5**, a013243

35. Shimosawa, O., Sakaguchi, M., Ogawa, H., Harada, N., Mihara, K., and Omura, T. (1993) Core glycosylation of cytochrome P-450(arom). Evidence for localization of N terminus of microsomal cytochrome P-450 in the lumen. *J. Biol. Chem.* **268**, 21399-21402

8. Acknowledgments

I thank Ms. Miwa Tsukuda, Ms. Yuki Sakaguchi, and Ms. Michiyo Takahara for technical assistance. I would like to express my gratitude to Professor Sakaguchi for his intimate advice, encouragement throughout the work and the opportunity of this study. I am also grateful to Associate Professor, Yoshikazu Emi, and Assistant Professor, Yuichiro Kida for their kind directions and assistances. I also thank to members of Sakaguchi laboratory for a lot of advice, technical support, and helpful cooperation.

9. Supplemental Figures

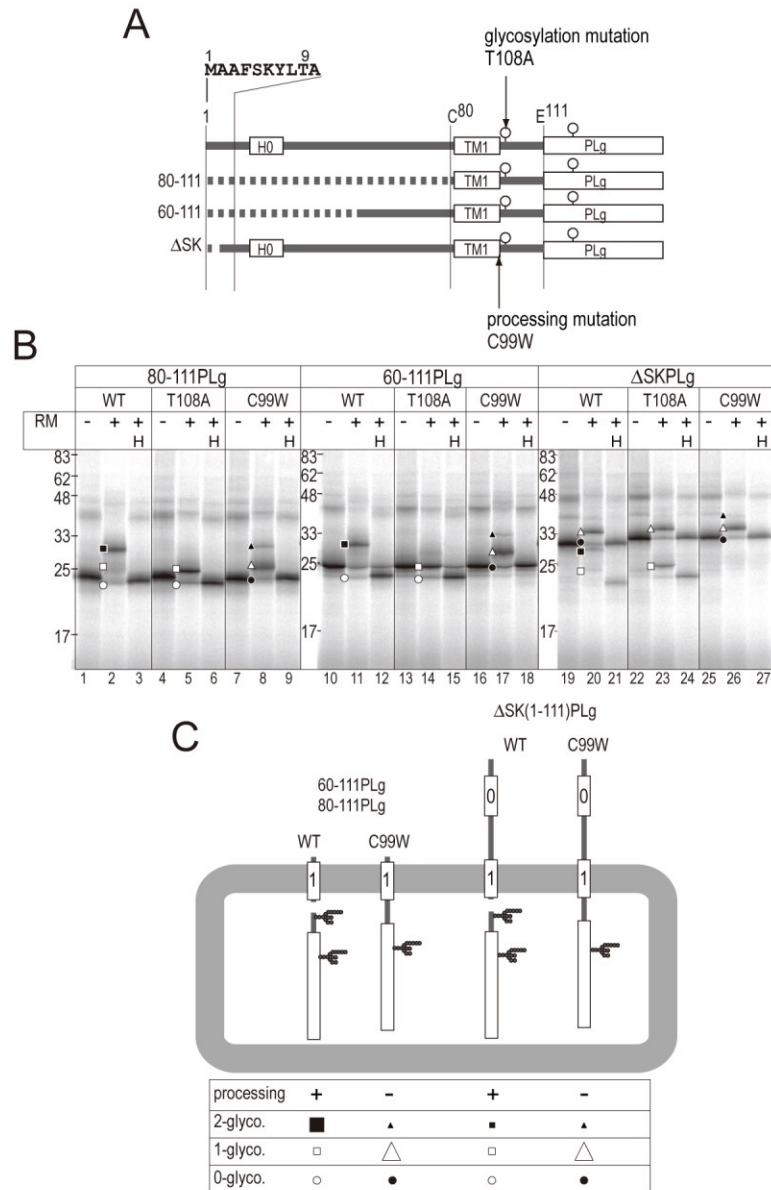


Figure S1. Processing and glycosylation of model proteins.

(A) To address the multiple forms observed in the presence of RM, the possible processing site Cys⁹⁹-Asp¹⁰⁰ anticipated by the SignalP 3.0 Server (24) and the potential glycosylation site (Asn¹⁰⁶) after the TM1 were silenced by point mutations, C99W and T108A, respectively. (B) The models were synthesized *in vitro* in the absence and presence (+) of RM. Aliquots were treated with EndoH under denaturing conditions. The products were subjected to SDS-PAGE and image analysis. The processed-diglycosylated form (closed square),

processed-monoglycosylated form (open square), processed-nonglycosylated form (open circle), unprocessed-nonglycosylated form (closed circle), unprocessed-monoglycosylated form (open triangle), and unprocessed-diglycosylated form (closed triangle) are indicated. With the glycosylation site mutation (T108A), the largest bands (closed squares) of the 60-111 and 80-111 constructs were not observed and the smaller forms (open squares) were enhanced (lanes 5 and 14), indicating that the largest forms were glycosylated at the Asn¹⁰⁶. The smaller forms were shifted down by EndoH treatment, indicating that the largest and smaller forms were diglycosylated and monoglycosylated products, respectively. On the processing site mutation (C99W), the unprocessed-diglycosylated forms were present in small amounts (closed triangles) and the unprocessed-monoglycosylated forms (open triangles) became dominant (lanes 8 and 17). The processed form observed after the EndoH-treatment disappeared and in turn unprocessed nonglycosylated forms appeared (lanes 9 and 18). In the case of the 60-111 and 81-111 fusion proteins, the TM1 segments were processed by signal peptidase and the processed forms were diglycosylated. In contrast, glycosylation site mutation (T108A) did not affect the monoglycosylated form of the Δ SK-PLg (open triangle) but rather the processed product (closed square) converged on the smaller one (open square; lanes 20 and 23). The largest major product (open triangle) was glycosylated only in the PLg domain. The minor product indicated by the closed square was the processed diglycosylated form. The processing mutation (C99W) did not affect the monoglycosylation (open triangle) of the Δ SK-mutant and the processed form was not observed after EndoH-treatment (lane 27). (C) Processing and glycosylation status in the membrane. In the absence of the N-terminal large portion, the TM1 segment was processed and the product was diglycosylated. In the presence of the N-terminal portion, the product was hardly processed and the unprocessed form was only monoglycosylated. The Asn¹⁰⁶ glycosylation site was glycosylated only when the TM1 segment was processed by the signal peptidase. In the bottom panel, relative amount of each form is indicated by the size of the symbols.

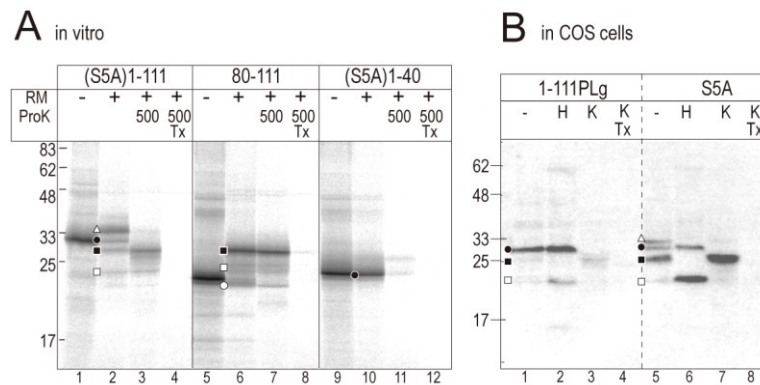


Figure S2. Membrane topology of the model proteins

(A) Membrane topology was probed by ProK treatment. Cell-free translation products were extensively digested with ProK (500 $\mu\text{g/ml}$) in the absence or presence of Triton X-100 (Tx lanes). The (S5A)1-111 construct was partially degraded and a large portion was resistant to ProK (lane 3), indicating that only the N-terminal portion was accessible to ProK. The membrane-protected fragments exhibited similar mobility to that of the 80-111 fusion protein (lane 7, closed square). The 80-111 fusion protein was fully resistant to ProK, indicating that there was no segment accessible to the cytoplasmic ProK. On the other hand, the S5A mutant of 1-40PLg was not glycosylated and fully degraded by ProK. The TM1 segment spans the membrane and the N-terminal segment was on the cytoplasmic side. The symbols are the same as shown in Fig. S1. (B) The (S5A)1-111 construct was mainly processed and diglycosylated in the living COS7 cells. The model proteins were expressed in COS7 cells in the presence of MG132 for 9 h. Cells were permeabilized with a low concentration of digitonin (25 $\mu\text{g/ml}$) in the culture dishes and aliquots were treated with ProK (K lanes) in the absence or presence of Triton X-100 (Tx lanes). Other aliquots were treated with EndoH under denaturing conditions (H lanes). EndoH treatment indicated that two products were glycosylated. The major band (closed square) is the processed-diglycosylated form and the largest band (open triangle) is the unprocessed-monoglycosylated form. The product glycosylated *in vitro* is larger than that *in vivo*, as previously observed (35), likely due to sugar trimming in COS7 cells. Upon ProK treatment, the major processed-diglycosylated form was fully resistant as observed in the

cell-free system (lane 7). These results indicated that the TM1 segment spanned the ER membrane.